

## LITERATURE CITED

- Allen, R. F., and C. M. Biggin, "Longitudinal Flow of a Lenticular Liquid Filament down an Inclined Plane," *Phys. Fluids*, **17**, 287 (1974).
- Bentwich, M., "Two-Phase Axial Laminar Flow in a Pipe with Naturally Curved Interface," *Chem. Eng. Sci.*, **31**, 71 (1976).
- Goodrich, F. C., "The Mathematical Theory of Capillarity," *Proc. Royal Soc.*, **A260**, 481 (1961).
- Kantorovich, L. V., and V. I. Krylov, *Approximate Methods of Higher Analysis*, Noordhoff, Groningen (1958).
- Kern, J., "Zur Hydrodynamik der Rinnsale," *verfahrenstechnik*, **3**, 425 (1969).
- , "Phenomena and Flow Regimes in Rivulet Flow," submitted to *J. Fluid Mech.* (1975).
- Morse, P. M., and H. Feshbach, *Methods of Theoretical Physics*, Chapt. IV, McGraw-Hill, New York (1953).
- Rayleigh, Lord, "On the Theory of the Capillary Tube," *Proc. Royal Soc.*, **A92**, 184 (1915).
- Towell, G. D., and L. B. Rothfeld, "Hydrodynamics of Rivulet Flow," *AIChE J.*, **12**, 972 (1966).

Manuscript received December 30, 1975; revision received May 4 and accepted May 5, 1976.

# Electropolarization Chromatography

JOAQUIM F. G. REIS

and

E. N. LIGHTFOOT

Department of Chemical Engineering  
University of Wisconsin  
Madison, Wisconsin 53706

The utility of electropolarization chromatography for fractionation of native protein mixtures is examined both mathematically and experimentally.

Mathematical prediction based on a simplified but basically realistic model of this process suggests it to be very promising for both analytical and preparative purposes.

This expectation is borne out by tests with well-defined proteins in single ultrafiltration fibers. The major observed departure from model prediction is an unexpectedly sharp increase in retardation at a critical voltage specific to the protein and composition of the carrier electrolyte. This permits sharper separations than previously expected and is thus favorable.

## SCOPE

A new process, electropolarization chromatography or EPC, is proposed for the fractionation of native proteins. This process is described qualitatively and in terms of a relatively simple mathematical model which adequately encompasses most of its characteristic behavior. Pre-

liminary experimental results are presented which support the model but also show the possibility of greatly enhanced separation effectiveness under mild process conditions in simple equipment constructed from commercially available materials.

## CONCLUSIONS AND SIGNIFICANCE

EPC is inherently superior to such processes as free-flow electrophoresis from the standpoints of resolution, removal of ohmic heat, and suppression of free convection. It can be carried out in very simple equipment at

modest voltages, and it offers unusual flexibility, both in choice of operating conditions and scale. Preparative separations appear to be feasible upwards from tens of micrograms without major scale-up problems.

Electrophoresis has been known to be a powerful and flexible means for separating proteins since the pioneering experiments of Tiselius (1937), and it has been used for many years as an analytical tool. It has not yet been very successful on a preparative scale, however, and we have shown (Reis et al., 1974) that this is in part because of excessive convectively induced dispersion (Taylor diffusion). It is in fact clear from our analysis that high resolution will inevitably be accompanied by prohibitive levels of ohmic heating in such processes as free-flow electrophoresis (Hannig, 1964, 1969).

We have accordingly proposed (Lee et al., 1974) as an alternate to free-flow electrophoresis (FFEP) a process we now call electropolarization chromatography (EPC).\*

\* We have referred to this in the past as electrophoretic single-phase chromatography, and Giddings has used electrophoretic field-flow fractionation. The term EPC, proposed by Peter Rigopoulos of Amicon Corporation, is more compact and emphasizes the key role of polarization.

In this process, described more completely below, pulses of protein mixtures are added to a carrier solution flowing in a cylindrical duct of convenient cross section. The proteins are then segregated into the neighborhood of the duct wall and hence into slower moving regions of the carrier by the presence of a transverse electric field. The effective axial velocity of each component of the feed is determined by the degree of segregation, and this in turn depends on the electrochemical nature of the protein, in particular its charge density.

We show in a separate mathematical analysis (Reis et al., 1976) that EPC is frequently much superior to FFEP, from the standpoint of potential resolving power, removal of ohmic heat, and control of free convection. We further show that ducts of circular cross section are particularly promising for control of geometry and flow distribution, for ease of heat removal, and for simplicity of manifolding in large systems.

The idea of polarization induced protein fractionation goes back at least to Kirkwood (1941), who then proposed electrophoresis convection as an analogue of the Clusius column. In the proposed separation method, electromigration replaced thermal diffusion. The nonuniform flow field in the narrow channel of the separator was due to free convection. Essentially to speed up the process, Bier (1957) proposed that forced convection (laminar flow) should be used. In Kirkwood's equipment the feed occupied the whole system, initially, and in Bier's design the feed was supplied continuously. In both cases, then, only binary separations could be carried out. Giddings (1966) suggested that field-flow separators could be used for multi-component fractionation if a feed pulse was used instead. Caldwell et al. (1972) reported multicomponent fractionations obtained with an electrical field-flow fractionator. These authors used a field pulse in a narrow channel, where a parabolic convection profile is combined with a transversal electrical field. Lee et al. (1974) proposed that pressure diffusion could be used as an effective cross field and that electrical field flow fractionation could advantageously be carried out in a hollow fiber.

The purposes of this paper are to explore the potential utility of hollow-fiber EPC by mathematical analysis and to assess its feasibility by selected experiments in single-fiber test systems. These tests are particularly important, since relatively little is yet known about the transport properties and chemical stability of proteins in highly concentrated mixed solutions or the sorptive properties of the available fibers.

## PROCESS DESCRIPTION

Hollow-fiber EPC is most simply described in terms of the single-fiber system of Figure 1. This consists essentially of an ultrafiltration fiber, here of circular cross section, bathed in a circulating buffer solution and subjected to a transverse electric field.

In operation, carrier electrolyte flows through the fiber lumen (that is, in the  $z$  direction) continuously, and a pulse of the protein mixture to be separated is introduced at the feed end ( $z = 0$ ) to initiate the separation.

The electric field results in a polarization of each protein, that is, a nonuniform distribution over the column cross section, as indicated in the figure. The axial velocity of a protein pulse may then be represented as

$$u_i = \frac{\int_S c_i v \, ds}{\int_S c_i \, ds}$$

The velocity  $u_i$  is then the velocity of the center of mass of species  $i$ .

It will be seen below that the retardation coefficient

$$r_i \equiv \langle v \rangle / u_i$$

where  $\langle v \rangle$  is the flow average carrier velocity, is always greater than unity for a finite field and that  $r_i$  increases with the degree of polarization. Separation of any two species is possible when their retardation coefficients differ.

The retardation coefficient is in fact the process characteristic of greatest interest in determining the feasibility of separation, and the remainder of this paper is devoted primarily to its prediction and measurement.

Axial dispersion of solute pulses is also important in determining the resolving power of the process. We shall show in a later paper that axial dispersion is sharply reduced by polarization and hence that the inherent resolving power of EPC columns is high. We do not discuss

this point further here, however, because dispersion in our present apparatus is dominated by the monitoring apparatus used.

## MATHEMATICAL MODELING

The general description of the concentration distribution of species  $i$  in the system schematically represented in Figure 1 is

$$\frac{\partial c_i}{\partial t} + v_0 \left[ 1 - \frac{x^2 + y^2}{R^2} \right] \frac{\partial c_i}{\partial z} + m_i \left[ E_x \frac{\partial c_i}{\partial x} + E_y \frac{\partial c_i}{\partial y} \right] = \mathcal{D}_{im} \left[ \frac{\partial^2 c_i}{\partial x^2} + \frac{\partial^2 c_i}{\partial y^2} + \frac{\partial^2 c_i}{\partial z^2} \right] \quad (1)$$

The first boundary condition which goes with Equation (1) is the statement of zero net flux normally to the wall for each polyelectrolyte; that is

$$m_i \left[ \frac{x}{R} E_y + \frac{y}{R} E_x \right] c_i = \mathcal{D}_{im} \left[ \frac{x}{R} \frac{\partial c_i}{\partial x} + \frac{y}{R} \frac{\partial c_i}{\partial y} \right] \quad \text{at } x^2 + y^2 = R^2 \quad (2)$$

The second boundary condition is that the concentration distribution is symmetric with respect to the  $z$ - $y$  plane.

The initial condition does not have to be specified for the level of description to be presented in this paper.

The spatial distribution of the electrical field inside the hollow fiber is now discussed. The electrical field is assumed to be uniform and directed along the  $y$  axis when infinitely far from the hollow fiber. The axis of the hollow fiber is perpendicular to the  $y$  direction, and the deformation of the electrical field introduced by the fiber depends only on the electrical conductivity of its wall. The simplest situation results from an isotropic wall. In this case the electrical field inside the fiber is uniform and directed along the  $y$  axis (Lee et al., 1974). The ratio between the electrical field inside and infinitely far outside the fiber is

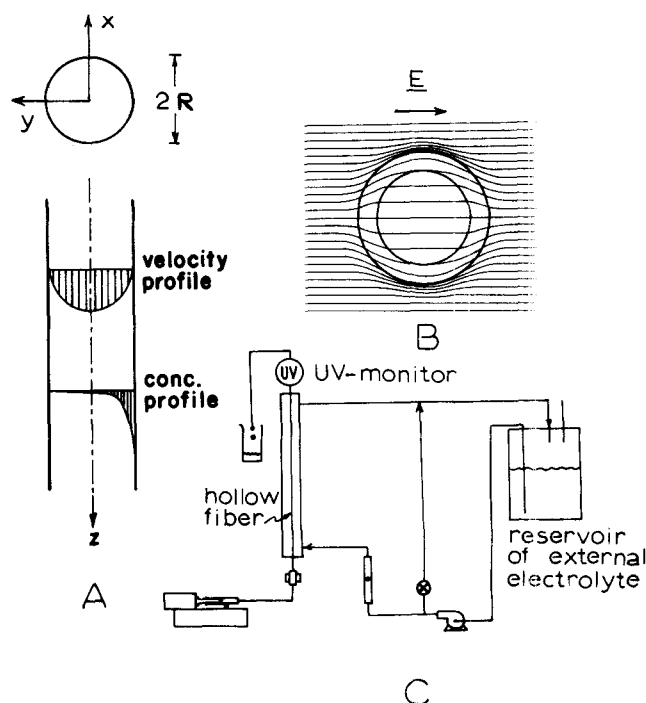


Fig. 1. Hollow-fiber EPC: (A) coordinate system, convection velocity profile and equilibrium concentration profile in the hollow fiber. (B) distortion of the electrical force lines due to the presence of an isotropic cylindrical duct. (C) sketch of the experimental setup.

$$\frac{E_{\text{inside}}}{E_{\text{outside}}} = \frac{1}{\left[ \frac{1+\gamma}{2} \right]^2 + \left[ \frac{1-\gamma}{1+\frac{\delta}{R}} \right]^2} \quad (3)$$

where  $\delta/R$  is the ratio between the thickness of the wall and the internal radius of the fiber (see Figure 1B).

In fact, anisotropic hollow fibers have a thin inner skin where the field is essentially radial. The uniform electrical field inside the hollow fiber is then, at best, an approximation of the real system. However, given the fact that the thickness of the inner skin is of the order of magnitude of one thousandth of the radius of the hollow fiber, it seems reasonable that if the center of mass of one species is not too close to the wall, the assumption of uniform electrical field is satisfactory. It is shown later on that under typical operation conditions, the distance of the center of mass of a highly retarded species to the wall is about fifty times larger than the thickness of the inner skin.

If the electrical field is uniform and directed along the  $y$  direction, Equations (1) and (2) reduce to

$$\begin{aligned} \frac{\partial c_i}{\partial t} + v_0 \left[ 1 - \frac{x^2 + y^2}{R^2} \right] \frac{\partial c_i}{\partial z} + m_i E_y \frac{\partial c_i}{\partial y} \\ = \mathcal{D}_{im} \left[ \frac{\partial^2 c_i}{\partial x^2} + \frac{\partial^2 c_i}{\partial y^2} + \frac{\partial^2 c_i}{\partial z^2} \right] \end{aligned} \quad (4)$$

and

$$m_i \left[ \frac{x}{R} E_y \right] c_i = \mathcal{D}_{im} \left[ \frac{x}{R} \frac{\partial c_i}{\partial x} + \frac{y}{R} \frac{\partial c_i}{\partial y} \right] \quad \text{at } x^2 + y^2 = R^2 \quad (5)$$

#### MOVEMENT OF THE CENTERS OF MASS OF THE SOLUTES

The velocity of the center of mass of species  $i$  is given by

$$u_i = \frac{\int_{-R}^{+R} \int_{-\sqrt{R^2-x^2}}^{+\sqrt{R^2-x^2}} \int_{-\infty}^{+\infty} c_i v \, dx dy dz}{\int_{-R}^{+R} \int_{-\sqrt{R^2-x^2}}^{+\sqrt{R^2-x^2}} \int_{-\infty}^{+\infty} c_i \, dx dy dz} \quad (6)$$

and it is then convenient to define a function  $f_i$  as

$$f_i \equiv \frac{\pi R^2 \int_{-\infty}^{+\infty} c_i \, dz}{\int_{-R}^{+R} \int_{-\sqrt{R^2-x^2}}^{+\sqrt{R^2-x^2}} \int_{-\infty}^{+\infty} c_i \, dx dy dz} \quad (7)$$

From Equations (6) and (7) it is clear that  $u_i$  and  $f_i$  are related through the equation

$$u_i = \frac{1}{\pi R^2} \int_{-R}^{+R} \int_{-\sqrt{R^2-x^2}}^{+\sqrt{R^2-x^2}} v f_i \, dy dx \quad (8)$$

When we introduce the following set of dimensionless variables

$$P\acute{e} = R \frac{v_0}{\mathcal{D}_{im}} \quad (9)$$

$$\tau = \frac{tv_0}{R} \cdot \frac{1}{P\acute{e}} \quad (10)$$

$$\epsilon_i = \frac{m_i E_y}{v_0} \cdot P\acute{e} \quad (11)$$

$$\eta = \frac{y}{R} \quad (12)$$

$$\chi = \frac{x}{R} \quad (13)$$

the general description [Equation (4)] becomes, in terms of  $f_i$

$$\frac{\partial f_i}{\partial \tau} + \epsilon_i \frac{\partial f_i}{\partial \eta} - \frac{\partial^2 f_i}{\partial \eta^2} - \frac{\partial^2 f_i}{\partial \chi^2} = 0 \quad (14)$$

When we represent by  $\bar{f}_i$  the steady state part of  $f_i$ , the equation

$$\epsilon_i \frac{\partial \bar{f}_i}{\partial \eta} - \frac{\partial^2 \bar{f}_i}{\partial \eta^2} - \frac{\partial^2 \bar{f}_i}{\partial \chi^2} = 0 \quad (15)$$

applies. The boundary condition which goes with Equation (15) is, from Equation (5)

$$\epsilon_i \bar{f}_i = \frac{\partial \bar{f}_i}{\partial \eta} + \frac{\chi}{\eta} \frac{\partial \bar{f}_i}{\partial \chi} \quad \text{at } \eta^2 + \chi^2 = 1 \quad (16)$$

Equation (15) can be solved by separation of variables, and  $\bar{f}_i$  turns out to be, simply

$$\bar{f}_i = \frac{\epsilon_i e^{\epsilon_i \eta}}{2I_1(\epsilon_i)} \quad (17)$$

where  $I_1$  is the hyperbolic Bessel function of order 1. The proportionality constant  $\epsilon_i/[2I_1(\epsilon_i)]$  was calculated from the normalization condition

$$\frac{1}{\pi R^2} \int_{-R}^{+R} \int_{-\sqrt{R^2-x^2}}^{+\sqrt{R^2-x^2}} \bar{f}_i \, dy dx = 1 \quad (18)$$

which follows immediately from Equation (7).

From Equation (17), the steady state value of the velocity of the center of mass of species  $i$  may be computed as

$$\bar{u}_i = \frac{2v_0}{\epsilon_i} \cdot \frac{I_2(\epsilon_i)}{I_1(\epsilon_i)} \quad (19)$$

where  $I_2$  is the hyperbolic Bessel function of order 2.

By defining a retardation coefficient  $r_i(E_y)$  as

$$r_i(E_y) = \frac{\left[ \text{velocity of the center of mass under the zero electrical field} \right]}{\left[ \text{velocity of the center of mass under the electrical field } E_y \right]} \quad (20)$$

it is, from Equation (19)

$$r_i(E_y) = \frac{\epsilon_i}{4} \cdot \frac{I_1(\epsilon_i)}{I_2(\epsilon_i)} = \frac{m_i E_y R}{4\mathcal{D}_{im}} \cdot \frac{I_1 \left[ \frac{m_i E_y R}{\mathcal{D}_{im}} \right]}{I_2 \left[ \frac{m_i E_y R}{\mathcal{D}_{im}} \right]} \quad (21)$$

For a hollow fiber with a 0.05 cm I.D., the retardation coefficients of albumin and gamma globulin with transport properties as in barbital 0.1M at pH 8.6 are plotted in Figure 2 as functions of the electrical field.

This distance of the center of mass of the species  $i$  from the  $x$  axis,  $Y_i$ , is

$$Y_i = R \frac{1}{\pi} \int_{-1}^{+1} \bar{f}_i \int_{-\sqrt{1-\eta^2}}^{+\sqrt{1-\eta^2}} d\chi d\eta$$

It follows, then, that in the large-time limit

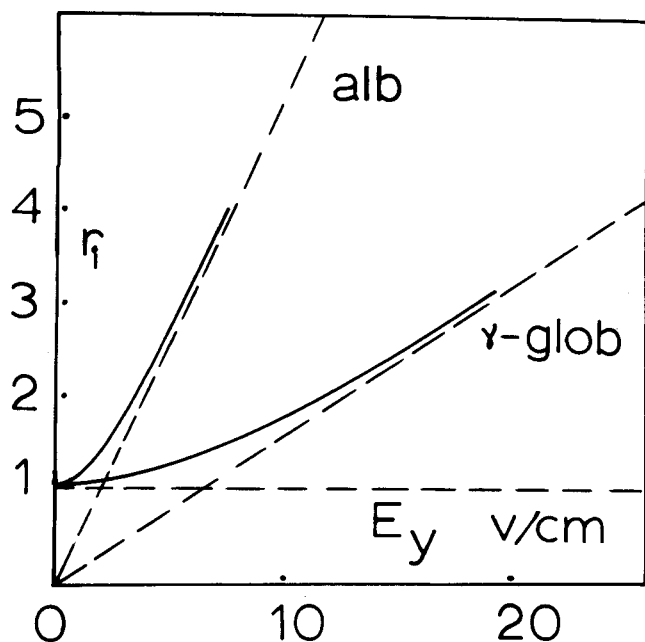


Fig. 2. The electrical field dependence of the retardation coefficient for human serum albumin ( $m = 5.92 \times 10^{-5} \text{ cm}^2/\text{V}\cdot\text{s}$ ;  $D = 6.1 \times 10^{-7} \text{ cm}^2/\text{s}$ ) and human gamma globulin ( $m = 1.2 \times 10^{-5} \text{ cm}^2/\text{V}\cdot\text{s}$ ;  $D = 4 \times 10^{-7} \text{ cm}^2/\text{s}$ ) in barbital 0.1M at pH 8.6, as predicted by the model presented in the text. The straight lines represent asymptotes for zero electrical field ( $r_i \rightarrow 1$ ) and large

$$\text{electrical field } \left( r_i \rightarrow \frac{m_i}{D_{im}} \cdot \frac{R}{4} \cdot E_y \right).$$

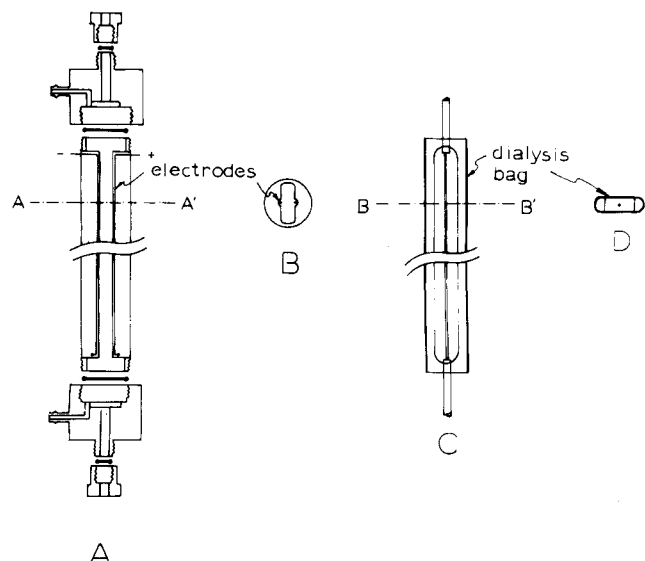


Fig. 3. Apparatus for hollow-fiber EPC: (A) outer shell, made of plexiglas, with platinum wire electrodes. (B) section AA' showing the electrodes. (C) fiber cartridge with hollow fiber, wrapped in the dialysis bag. (D) section BB'.

$$\frac{Y_i}{R} = \frac{2 \epsilon_i}{2 \pi I_1(\epsilon_i)} \int_{-1}^{+1} e^{\epsilon_i \eta} \sqrt{1 - \eta^2} d\eta$$

or

$$\frac{Y_i}{R} = \frac{I_2(\epsilon_i)}{I_1(\epsilon_i)} \quad (22)$$

In a hollow fiber with a 0.05 cm I.D., subjected to a transverse electrical field of 10 V/cm, for transport properties as in barbital 0.1 M at pH 8.6, Equation (22) gives, for albumin

$$1 - \frac{Y_{A1}}{R} = 0.056$$

and for gamma globulin

$$1 - \frac{Y_{\gamma\gamma}}{R} = 0.216$$

If the thickness of the inner skin of the hollow fiber is one thousandth of the radius, the distance of the center of mass to the wall is 56 times the thickness of the skin for albumin and 216 times for gamma globulin. This shows that under typical conditions the species are not too compressed to the wall. This result was used to support the assumption of uniform internal electrical field.

## EXPERIMENTAL APPARATUS AND PROCEDURE

To test the validity of the above model, experiments were made with well-defined proteins in the apparatus of Figure 3.

This apparatus is an implementation of Figure 1 to facilitate operation and replacement of test fibers and to keep the gas generated at the electrodes from the neighborhood of the fibers.

All fibers were supplied by the Amicon Corporation\* and were either of their P5 type or experimental variations thereof. Each fiber was 0.43 mm internal diameter, 50 cm long, and had a nominal molecular weight cutoff of  $5 \times 10^3$ . The hollow fiber was isolated from the platinum wire electrodes by a dialysis bag. The carrier solution was pushed through an injection valve, the hollow fiber, and an UV flow cell by means of a Harvard infusion pump. The electrolyte which filled the column was circulated through a large reservoir, in an open system. A chromatronix injection valve with a 10  $\mu\text{L}$  sample chamber was used to introduce the feed pulse; a Perkin-Elmer L-55 spectrophotometer with a 8  $\mu\text{L}$  flow cell was used for protein monitoring; an electronic measurements power supply, in voltage control mode, was used to provide the electrical field between the electrodes, placed 1.7 cm apart.

Solutions of the following proteins were run in our polarization chromatography column: human serum albumin 4 times crystallized, from Nutritional Biochemical Corporation; bovine gamma globulin, fraction II, from NBC; chymotrypsinogen A, from Aldrich Chemical Company. Human IgG and human IgM were graciously made available by Dr. H. Deutsch from the Physiological Chemistry Department of the University of Wisconsin. Three different buffers were used to prepare the protein solutions: barbital, from Fisher Scientific Company, at pH 8.6; tris (tris-hydroxymethylaminomethane), from Sigma Chemical Company, at pH 8.3; and sodium succinate, from Fisher Scientific Company, at pH 5.0. The ionic strength of the buffers was 0.001 M.

The flow rate of the carrier solution was 12.5  $\mu\text{L}/\text{min}$  in most runs. With higher flow rates (for example, 60  $\mu\text{L}/\text{min}$ ), steady state was not reached in the available length of the column, resulting in only partial retardation of the injected pulse by the electrical field. Slower flows produce better separations at the expense of experimental times longer than 2 hr.

The experiments reported in this paper are of two types: determination of the retardation coefficient, for a given protein and buffer, as a function of the electrical field for one or more fixed flow rates of the carrier solution; and separation of binary mixtures.

The electrical field inside the hollow fiber was calculated with the help of the model presented about for the dependence of the retardation coefficients on the electrical field. To do this, we assumed that the model applies at least for low retardation coefficients and that the electrical field prevailing inside the fiber is proportional to the applied voltage [Equation (3)]:

$$E_y = \alpha V \quad (23)$$

The retardation coefficients were calculated as the ratio of the differences in residence times, as in Equation (24):

$$r_i(E_y) = \frac{\theta_i(E_y) - \theta_c}{\theta_0 - \theta_c} \quad (24)$$

where

\* Amicon Corporation, Lexington, Massachusetts.

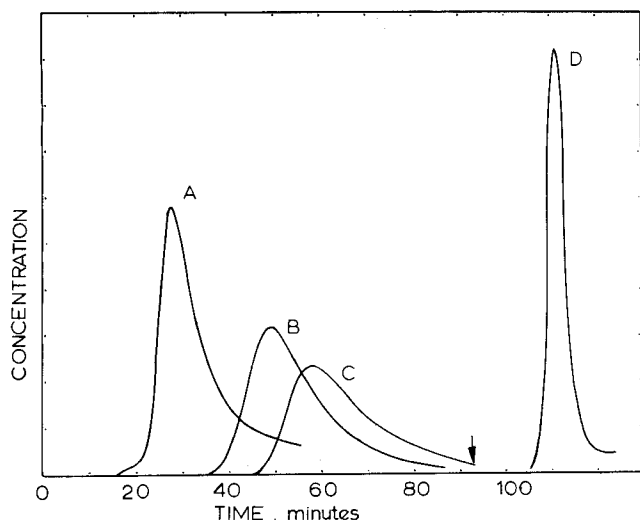


Fig. 4. Retardation and electroretention data for chymotrypsinogen A in tris 0.001M at pH 8.3. The electrical field was kept constant for 93 min after the injection and was then turned off. The flow rate was 12.5  $\mu\text{L}/\text{min}$ . In this figure the absorbance at 282 nm was recorded as a function of time: (A)  $E_y = 0$  V/cm, 50  $\mu\text{g}$  pulse. (B)  $E_y = 17$  V/cm, 50  $\mu\text{g}$  pulse. (C)  $E_y = 22$  V/cm, 50  $\mu\text{g}$  pulse. (D)  $E_y = 24$  V/cm, 50  $\mu\text{g}$  pulse.

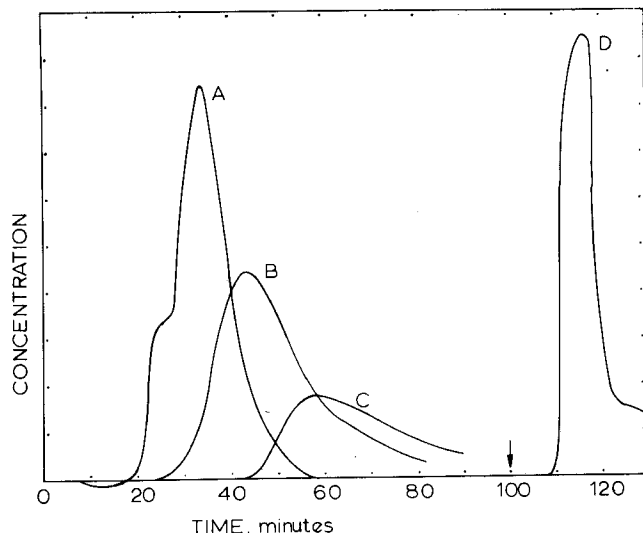


Fig. 5. Retardation and electroretention data for bovine gamma globulin in sodium succinate 0.001M at pH 5.0. The electrical field was kept constant for 100 min after the injection and was then turned off. The flow rate was 12.5  $\mu\text{L}/\text{min}$ . Each pulse contained 50  $\mu\text{g}$  of gamma globulin. In this figure the absorbance at 282 nm was recorded as a function of time: (A) 0 V/cm. (B) 10.5 V/cm. (C) 13.5 V/cm. (D) 16 V/cm.

$r_i(E_y)$  = retardation coefficient of species  $i$ , under the electrical field  $E_y$

$\theta_i(E_y)$  = residence time recorded for a pulse of species  $i$ , under the electrical field  $E_y$

$\theta_c$  = residence time recorded for a pulse of protein injected into the connectors only (system identical to the separation system up to the inlet to the hollow fiber and down after the outlet from the hollow fiber, with the inlet connected directly to the outlet)

$\theta_0$  = residence time for a pulse of protein, under zero electrical field

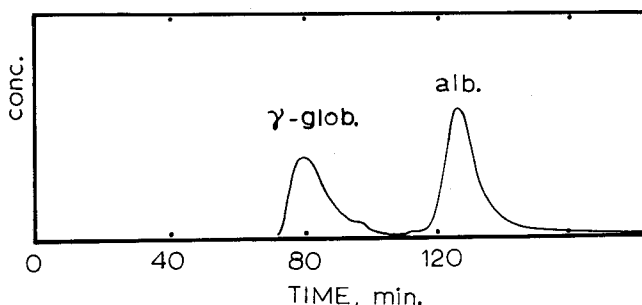


Fig. 6. Separation of human serum albumin from bovine gamma globulin in tris 0.001M at pH 8.3, under 7 V/cm. The carrier flow rate was 4.9  $\mu\text{L}/\text{min}$

The parameter  $\alpha$  was adjusted to optimize the fit of the model to the experimental retardation coefficients for human serum albumin and human gamma globulin (IgG), both at pH 8.6 in barbital. Only retardation coefficients below 4 (voltages up to 38 V) were used in the fitting procedure. The value of  $\alpha$  thus determined for P5 fibers was 0.29. This value of  $\alpha$  also provided a good fit for chymotrypsinogen A in tris at pH 8.3. For the experimental tighter hollow fibers, the parameter  $\alpha$  takes values which are lower (from 0.2 to 0.26) and not as consistent (from fiber to fiber) as for P5 fibers.

## RESULTS

The primary data are plots of exit optical density, for all practical purposes proportional to protein concentration, as a function of time. These are shown in Figures 4 to 7 for representative runs. These, in turn, can be used to determine  $r_i$  as a function of the calculated electrical field, as previously discussed. Figures 4 and 5 show part of the primary data on chymotrypsinogen A and IgG used in the construction of Figure 8. They can also be used to compare separations of protein mixtures with the behavior of single proteins. This is done in Figure 7 for the immuno-globulin fractions IgG and IgM. At the end of this section, the material balance of the injected samples is discussed.

### Retardation Coefficient vs. Electrical Field

The model represented in Figure 2 satisfactorily predicts the experimental data for low voltages. This enables us to calculate the parameter  $\alpha$  as discussed above and thus convert applied voltages into effective electrical fields. The value of  $\alpha$  computed from human serum albumin and human gamma globulin data in barbital 0.001 M at pH 8.6 provides a good fit for chymotrypsinogen A and

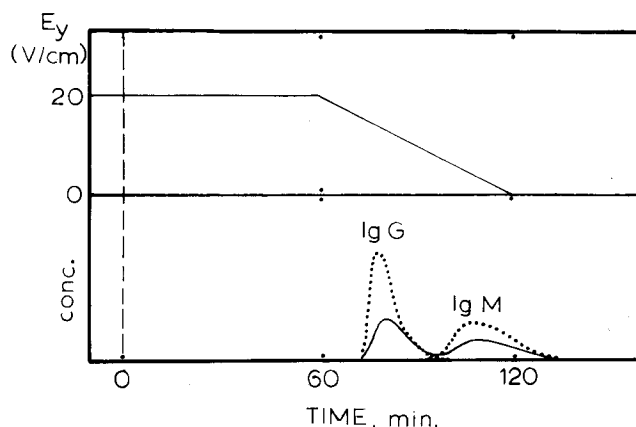


Fig. 7. Separation of IgM from IgG. The full line corresponds to the mixture, and the dotted lines correspond to separate injections of the components of the mixture.

bovine gamma globulin for low electrical fields (up to 8 V/cm for bovine gamma globulin at pH 5.0 and 18 V/cm for chymotrypsinogen A at pH 8.3).

At higher electrical fields, however, the experimental results depart sharply from the prediction, as illustrated in Figure 8. These results show that above a species dependent electrical field, the injected pulse (typically 50  $\mu\text{g}$ ) is totally retained on the hollow fiber's inner wall. This electroretention phenomenon has the following general characteristics: it is small at electrical fields below some

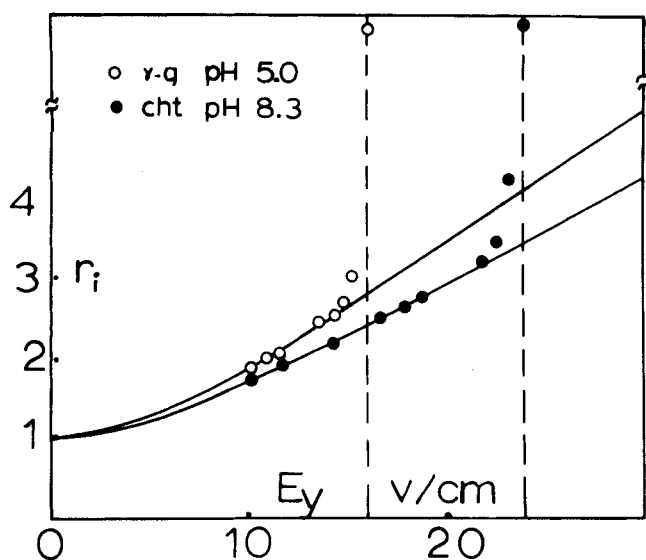


Fig. 8. Retardation coefficients vs. electrical field for chymotrypsinogen A at pH 8.3 in tris 0.001M and bovine gamma globulin at pH 5.0 in sodium succinate 0.001M. The values for the electrical field were calculated from applied voltages by means of Equation (21) with  $\alpha = 0.29 \text{ cm}^{-1}$ , obtained from calibration with human serum albumin and IgG in barbital 0.001M at pH 8.6. The values for  $m_i/D_{im}$  used to plot the theoretical curves were  $30 \text{ V}^{-1}$  for gamma globulin and  $25 \text{ V}^{-1}$  for chymotrypsinogen A. The figure shows that after some critical electrical field there is a sharp departure of experimental data from the prediction. The two data points on top of the plot correspond to peaks which were recovered only after the voltage was turned to zero.

species dependent critical level above which it grows rapidly up to saturation,\* and it is reversible for some species (chymotrypsinogen A and bovine gamma globulin) and at least partially reversible for others (human serum albumin).

#### Separations by Electropolarization Chromatography

In the absence of electrorotation, EPC may be carried out at constant electrical field to fractionate a mixture of polyelectrolytes with different values for the ratio  $m_i/D_{im}$  [see Equation (21)]. The same procedure can be used in the presence of electrorotation if the electrical field installed in the hollow fiber is smaller than the electrical fields of retention\* of the species to be separated. The separation of human serum albumin and bovine gamma globulin (Figure 6) is an example of simple EPC, carried out under constant electrical field. If higher electrical fields are to be used, then some kind of programming in time of the electrical field is required. EPC combined with electrorotation carried out with a programmed electrical field seems to be a very powerful and versatile separation technique. The separation of human IgG from human IgM, as illustrated in Figure 7, is an application of such technique.

#### Material Balance of the Injected Pulse

Pulses of  $50 \mu\text{g}$  of protein were injected into the separation system and into test systems where the hollow fiber was replaced by different ducts of the same length and comparable diameter but made up of different materials (polyethylene, Teflon, and stainless steel). The UV absorbance vs. time plots were compared. For each tested protein, with the exception of human serum albumin, the area under those plots was independent of the material

of the duct. With human serum albumin, the amount of protein recovered from the hollow fiber was consistently less than from any of the other ducts. The difference in recovery depended on the buffer solution being used, and it was small with tris (about 5%). Chymotrypsinogen A was quantitated by the Lowry method (Lowry, 1951) in the starting material (injection) and in the hollow fiber's effluent. Within the normal uncertainty of the method, the results show that the loss of injected protein is less than  $3 \mu\text{g}$  (6%).

The areas of the peaks under zero and nonzero electrical fields were also compared. If the peak due to electrorotation was included, the areas usually compared well. There was considerable loss when the protein was electrorotated for longer than 3 hr.

#### ACKNOWLEDGMENT

The authors are indebted for financial support to the National Science Foundation Grant ENG75/05456. In addition, J. F. G. Reis wishes to acknowledge the assistance provided by a Fundação Calouste Gulbenkian Fellowship.

#### NOTATION

$c$	=	molar concentration
$c_i$	=	molar concentration of species $i$
$D_{im}$	=	pseudo-binary diffusion coefficient of species $i$
$E_x$	=	$x$ component of the electrical field (V/cm)
$E_y$	=	$y$ component of the electrical field (V/cm)
$f_i$	=	distribution function as defined by Equation (7)
$\bar{f}_i$	=	steady state part of $f_i$
$I_n$	=	hyperbolic Bessel function of order $n$
$m$	=	electrophoretic mobility
$m_i$	=	electrophoretic mobility of species $i$
$Pé$	=	dimensionless parameter as defined by Equation (9)
$r_i$	=	retardation coefficient of species $i$
$R$	=	internal radius of the hollow fiber
$S$	=	cross section of the duct
$t$	=	time
$u_i$	=	velocity of the center of mass of species $i$
$\bar{u}_i$	=	steady state part of $u_i$
$v$	=	axial component of the molar-average velocity
$\langle v \rangle$	=	axial component of the flow-average velocity
$v_0$	=	maximum axial molar-average velocity
$V$	=	voltage applied across the electrodes (V)
$x$	=	rectangular coordinate as in Figure 1A
$y$	=	rectangular coordinate parallel to the internal electrical field
$Y_i$	=	distance of the center of mass of species $i$ from the $x$ axis
$z$	=	rectangular coordinate along the axis of the duct

#### Greek Letters

$\alpha$	=	proportionality constant as defined by Equation (23) ( $\text{cm}^{-1}$ )
$\gamma$	=	ratio between the electrical conductivities of the solution and the hollow-fiber wall
$\delta$	=	thickness of the hollow-fiber wall
$\epsilon_i$	=	dimensionless parameter as defined by Equation (11)
$\eta$	=	dimensionless coordinate as defined by Equation (12)
$\theta_i$	=	residence time of a pulse of species $i$
$\theta_0$	=	residence time under zero electrical field
$\theta_c$	=	residence time in the separation system, outside the hollow fiber
$\tau$	=	dimensionless time as defined by Equation (10)
$\chi$	=	dimensionless coordinate as defined by Equation (13)

\* Suggesting a sigmoidal curve for the sorption isotherm in electrorotation.

† We call electrical field of retention of one species the minimum electrical field which causes saturation of the wall with the said species.

## LITERATURE CITED

- Bier, M., "A New Principle of Preparative Electrophoresis," *Science*, **125**, 1084 (1957).
- Caldwell, K. D., L. F. Kesner, M. N. Meyers, and J. C. Giddings, "Electrical Field-Flow Fractionation of Proteins," *ibid.*, **176**, 296 (1972).
- Giddings, J. C., "A New Separation Concept Based on a Coupling of Concentration and Flow Nonuniformities," *Separation Science*, **1**, No. 1, 123 (1966).
- Hannig, K., "Eine Neuentwicklung der Trägerfreien Knotenirischen Elektrophorese," *Z. für Physiol. Chemie*, **338**, 211 (1964).
- , "The Application of Free-Flow Electrophoresis to the Separation of Macromolecules and Particles of Biological Importance," in *Modern Separation Methods of Macromolecules and Particles*, Theo Gerritsen, ed., Wiley-Interscience, New York (1969).
- Kirkwood, J. G., "A Suggestion for a New Method of Fractionation of Proteins by Electrophoresis-Convection," *J. Chem. Phys.*, **9**, 878 (1941).
- Lee, H-L, J. F. G. Reis, J. Dohner, and E. N. Lightfoot, "Single Phase Chromatography: Solute Retardation by Ultrafiltration and Electrophoresis," *AIChE J.*, **20**, No. 4, 776 (1974).
- Lowry, O. H., N. J. Rosebrough, and R. J. Randall, "Protein Measurement with the Folin Reagent," *J. Biol. Chem.*, **193**, 265 (1951).
- Reis, J. F. G., E. N. Lightfoot, and H-L Lee, "Concentration Profiles in Free-Flow Electrophoresis," *AIChE J.*, **20**, No. 2, 362 (1974).
- Reis, J. F. G., A. Shah, and E. N. Lightfoot, "Comparison between Electropolarization Chromatography and Free-Flow Electrophoresis," *ibid.*, to be proposed for publication.
- Tiselius, A., "A New Apparatus for Electrophoretic Analysis of Colloidal Mixtures," *Trans. Faraday Soc.*, **33**, 524 (1937).

Manuscript received January 19, 1976; revision received and accepted April 20, 1976.

# Design of An Ionic Lattice for Optimum Cation Diffusion

ELI RUCKENSTEIN

and

DADY B. DADYBURJOR

Faculty of Engineering and Applied Sciences  
State University of New York at Buffalo  
Buffalo, NY 14214

Varying the species and/or distance parameters of a lattice changes the activation energy of a particular species diffusing through it, thus allowing transport properties to be optimized. As an example, the activation energy of silver ions in  $\alpha$ -silver iodidelike structures was calculated as lattice properties were changed.

## SCOPE

The interaction between an ion moving in a lattice and another ion that is part of the lattice consists of coulombic, shell repulsion, induced dipole, and other energy terms. The mobile ion has a preferred path where the total energy, summed for all other ions, is always a minimum. This minimum energy as a function of the coordinate in the direction of motion has peaks and valleys. The difference between these extrema is an activation energy of transport of the ion and hence plays a part in determining the diffusivity and conductivity. Flygare and Huggins (1973) varied the ionic radius of the mobile cations through the  $\alpha$ -silver iodidelike lattice and found that the activation energy was a minimum (and hence ion transport was easiest) at an ionic radius close to the value determined experimentally for  $\text{Ag}^+$ . Hence, the observed high conductivity and diffusivity of silver ions in  $\alpha$ -silver iodide were directly related to the minimum in the activation energy for ionic transport.

In this work we suggest the inverse problem, the determination of lattice parameters so as to minimize the

activation energy of transport for a given species. This simple turnabout has vast potential applications. For example, it may be possible to design lattices for compounds to be used as solid electrolytes in fuel cells and batteries to minimize activation energies for mobile cations. At the present moment, the investigation and selection of these often complex materials is done on a case-by-case basis. (See, for instance, Hoshino, 1955; Geller and Lind, 1970; Geller, 1972.) A similar technique can also help in the design of an optimum catalyst. Batist et al. (1968) suggested that, at low temperatures, controlled diffusion of oxygen through the bismuth molybdate structure is important in the catalytic oxidation of 1-butene to butadiene. It may be possible to calculate the structure of a lattice that will give rise to the corresponding activation energy for oxygen diffusion and thus improve the selectivity of the catalyst.

As a simple example we consider below the determination of an  $\alpha$ -silver lattice to minimize transport of silver cations. This may be of value in the design of solid electrolytes (van Gool, 1974).